

Supporting Information for

A Superhydrophobic Bilayer Anisotropic Conductive Film with Improved Reliability for Electronic Interconnects

Wei Zhao^{a,b}, Guoxiang Zhang^{a,b}, Peipei Li^{a,b}, Libo He^c, Wenfeng Zhu^d, Lei Li^d, Houbu Li^d, Qi Zhang^e, Zhanchen Guo^{a*}, Xiaowei Liu^{f*}*

^a Shaanxi Key Laboratory of High-Orbits-Electron Materials and Protection Technology for Aerospace, School of Advanced Materials and Nanotechnology, Xidian University, Xi'an, Shaanxi, 710071, P.R. China.

^b State Key Laboratory of Electromechanical Integrated Manufacturing of High-performance Electronic Equipments, Xidian University, Xi'an, Shaanxi, 710071, P.R. China.

^c Shanghai Aerospace Resin based Composite Engineering Technology & Research Center, Shanghai Composites Science & Technology Co., Ltd., Shanghai, 201112, P.R. China.

^d Tubular Goods Research Institute, China National Petroleum Corporation & State Key Laboratory of Oil and Gas Equipment, Xi'an Shaanxi, 710065, P.R. China.

^e Zhengzhou Tobacco Research Institute, China National Tobacco Corporation, Zhengzhou, Henan, 450001, P.R. China.

^f Division of Physical Science and Engineering, King Abdullah University of Science and Technology, Thuwal 23955-6900, Kingdom of Saudi Arabia.

**Email: lip@xidian.edu.cn (P. Li), guozhanchen@xidian.edu.cn (Z. Guo), and xiaowei.liu@kaust.edu.sa (X. Liu)*

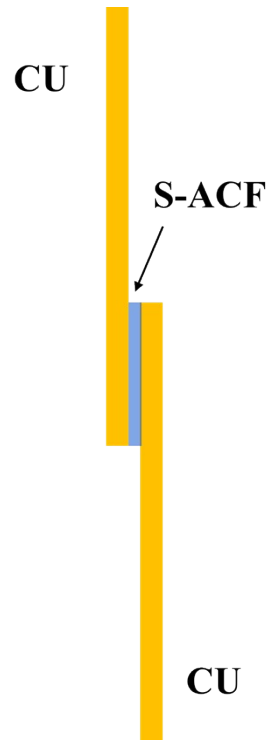


Figure S1. Bonding test sample schematic diagram, using two pieces of 40 mm×10 mm×0.3 mm copper sheets, sandwiching 10 mm×5 mm S-ACF in the middle, hot pressing for 10 minutes under 0.3 MPa and 150°C conditions, and then curing for one hour at 150°C, the bonding test sample can be prepared.

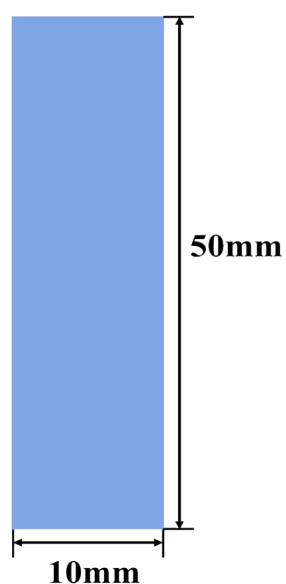


Figure S2. Schematic diagram of the tensile test sample. Cut the S-ACF into a 10 mm×50 mm rectangle and cure it at 150 °C for one hour to obtain the tensile test sample.

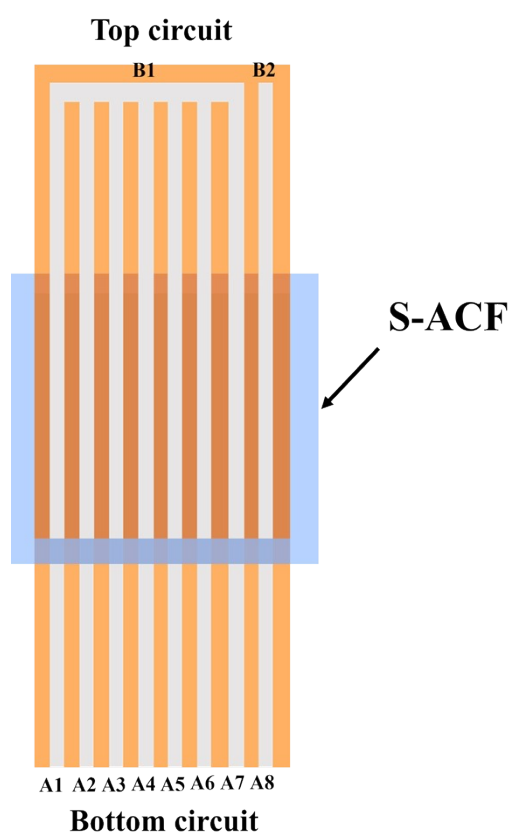


Figure S3. Ag electrodes were patterned on a PI film with an electrode spacing of 1 mm. The S-ACF was hot-pressed between the two electrodes at 150 °C under a pressure of 0.3 MPa, followed by curing at 150 °C for 1 h. The resistances measured between A1-A7 and B1 correspond to the Z-axis contact resistance, while the resistance measured between A8 and B1 represents the in-plane (X-Y) resistance. The electrode itself has an inherent resistance measured at 0.6 Ω.

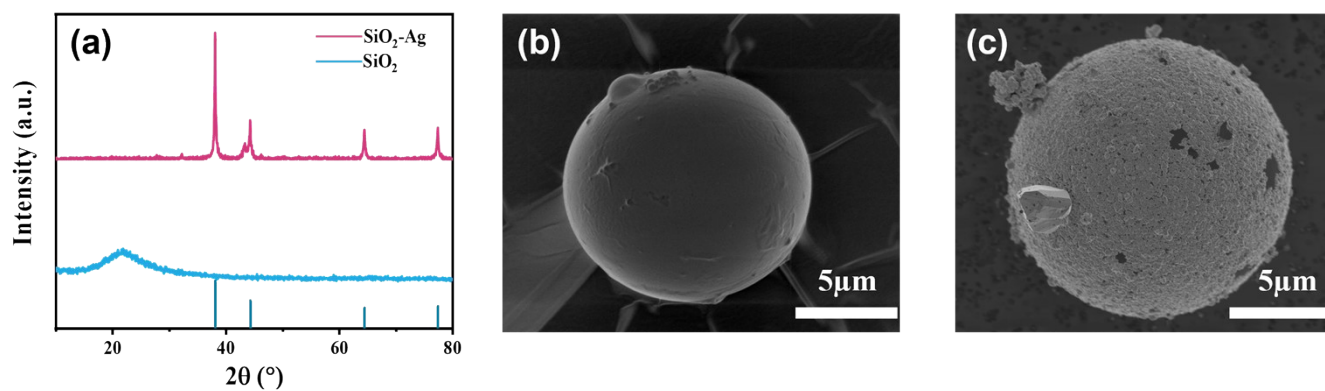


Figure S4. Characterization of SiO₂ spheres before and after silver coating: (a) X-ray diffraction patterns of uncoated SiO₂ and silver-coated SiO₂ spheres. (b, c) Scanning electron microscopy images of (b) the pristine SiO₂ spheres and (c) the silver-coated SiO₂ spheres.

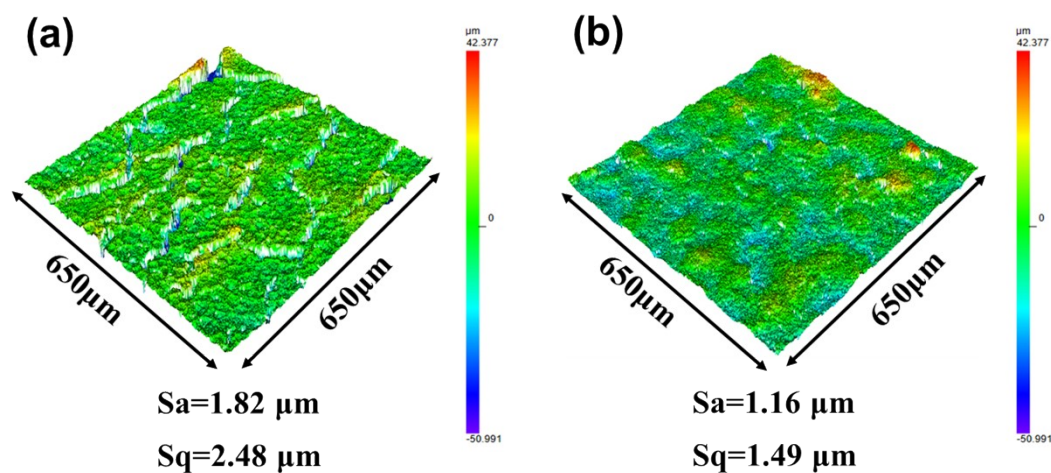


Figure S5. Laser scanning confocal microscopy (LSCM) images of S-ACF (a) with 150% pre-stretching and (b) without pre-stretching.

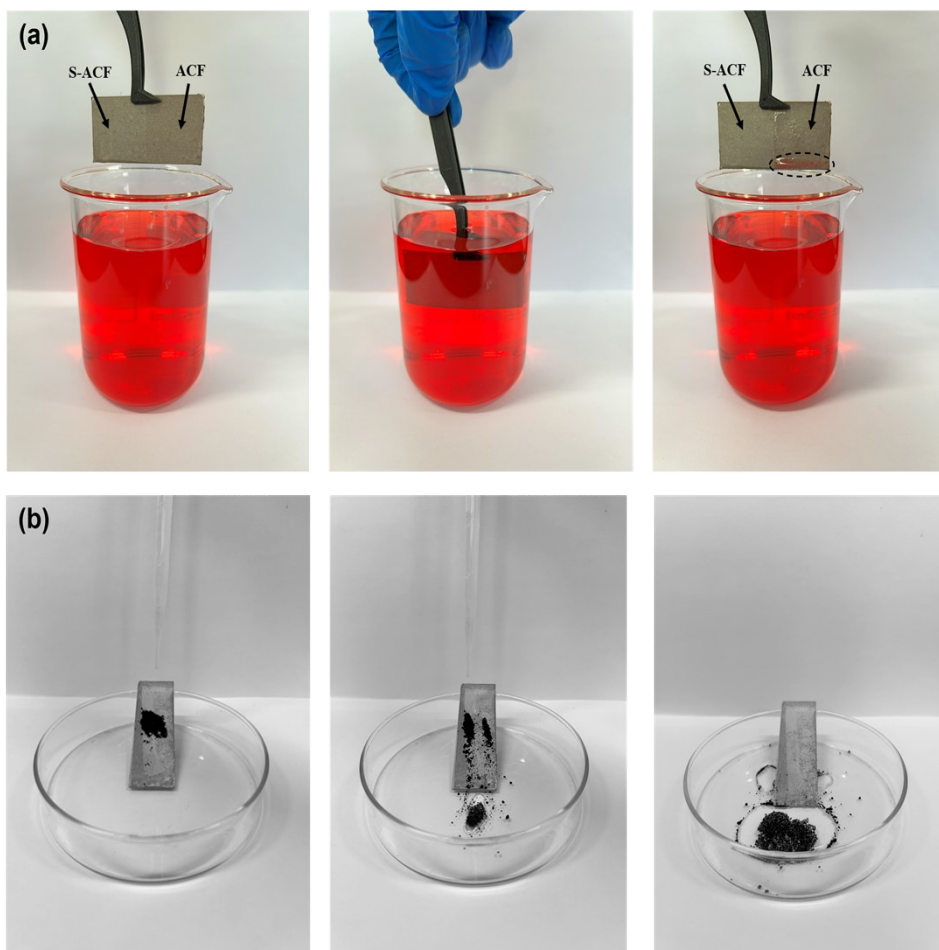


Figure S6. Anti-fouling and self-cleaning performance of the S-ACF. (a) Beading of a model ink contaminant on the hydrophobic S-ACF surface. (b) The subsequent removal of the contaminant, demonstrating the self-cleaning effect.

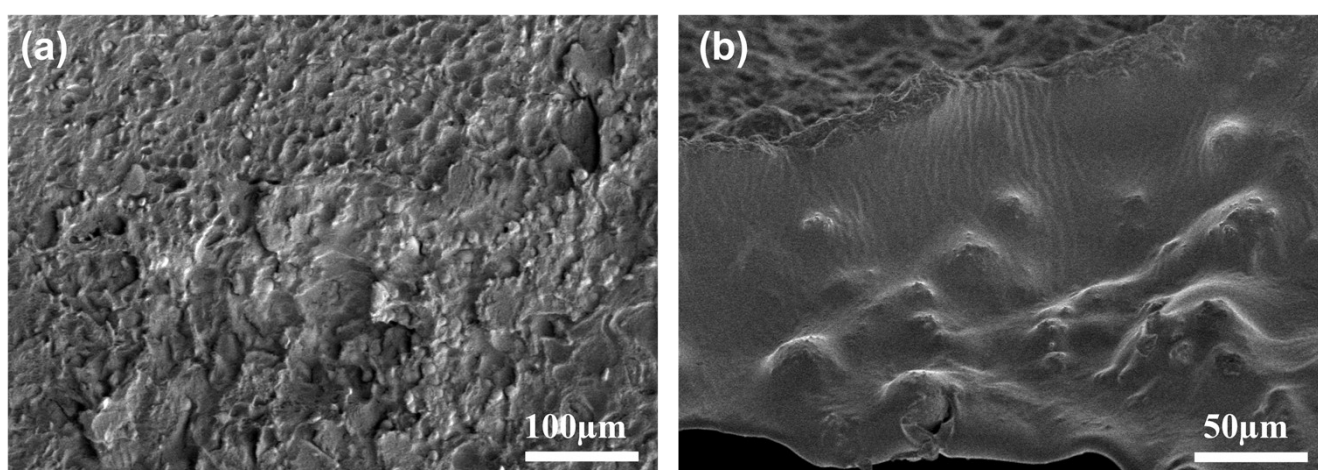


Figure S7. Mechanical test fracture surfaces SEM images of the S-ACF. (a) Fracture surfaces SEM micrograph of the S-ACF after the bonding test. (b) Fracture surfaces SEM micrograph of the S-ACF after the tensile test.

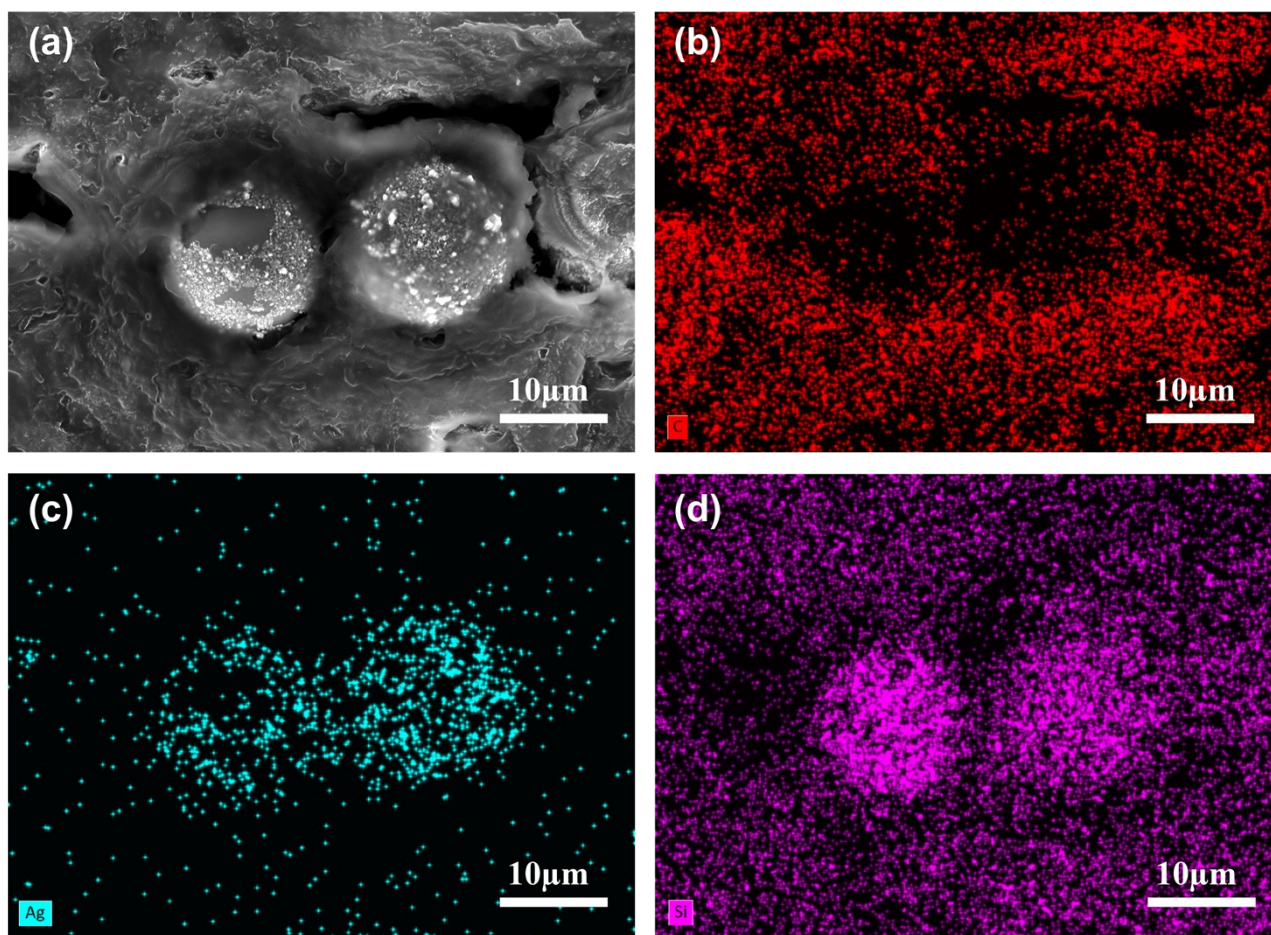


Figure S8. Surface SEM image and EDS elemental mapping of the S-ACF after hot pressing. (a) Surface SEM micrograph. (b–d) EDS elemental maps showing the distribution of (b) C, (c) Ag, and (d) Si.

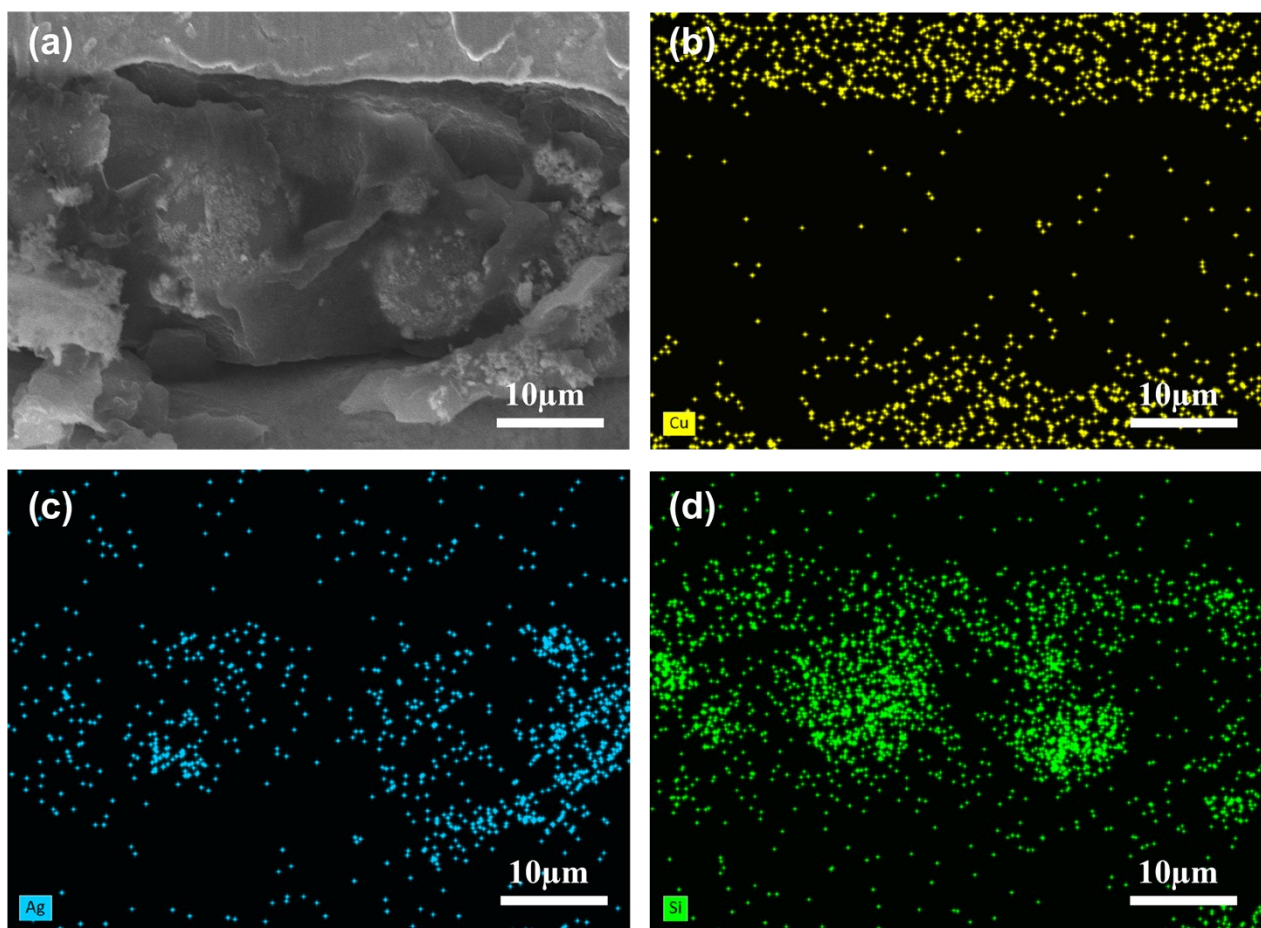


Figure S9. Cross-sectional SEM image and EDS elemental mapping of the S-ACF after hot-press curing between two Cu electrodes. (a) Cross-sectional SEM micrograph of the S-ACF laminated between two Cu electrodes after hot pressing. (b–d) EDS elemental maps showing the distribution of (b) Cu, (c) Ag, and (d) Si.

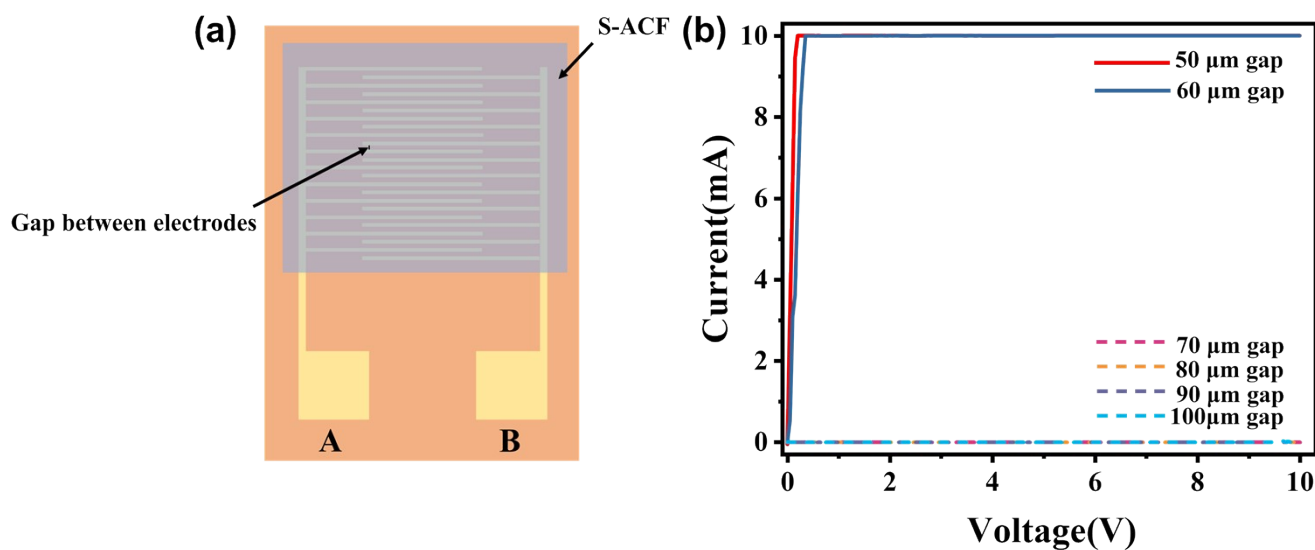


Figure S10. (a) Schematic illustration of the test setup for evaluating the electrical resolution of the S-ACF. The electrodes consist of a PI film and Au circuits, and the S-ACF was hot-pressed onto the electrodes and cured. (b) Test electrodes with electrode gaps of 50, 60, 70, 80, 90, and 100 μm were used to evaluate the electrical resolution of the S-ACF, and the corresponding I–V curves at different electrode gaps were measured

Table S1. Chemical formulations used to create superhydrophobic surfaces, showing the quantitative composition of each solution with different SiO₂ content.

SiO₂ (mg)	Cyclohexane (ml)	SEBS (mg)	Formula
100	100	200	1
150	100	200	2
200	100	200	3
250	100	200	4
300	100	200	5
400	100	200	6
450	100	200	7
500	100	200	8
550	100	200	9
600	100	200	10

Table S2. Evolution of Z-axis and XY-plane electrical resistance of the ACF during an accelerated aging test at 85°C and 85% relative humidity (RH).

Time (h)	Contact resistance (Z-axis, Ω)	Insulation resistance (XY plane, Ω)
0	1.58	$> 10^6$
24	1.61	$> 10^6$
48	1.67	$> 10^6$
72	1.74	$> 10^6$
96	1.83	$> 10^6$
120	2.04	$> 10^6$
144	2.27	$> 10^6$
168	2.88	$> 10^6$
192	3.04	$> 10^6$
216	3.21	$> 10^6$
240	3.53	$> 10^6$
264	3.67	$> 10^6$
288	3.61	$> 10^6$
312	3.83	$> 10^6$
336	4.01	$> 10^6$

Table S3. Evolution of Z-axis and XY-plane electrical resistance of the S-ACF during an accelerated aging test at 85°C and 85% relative humidity (RH).

Time (h)	Contact resistance (Z-axis, Ω)	Insulation resistance (XY plane, Ω)
0	1.64	$> 10^6$
24	1.67	$> 10^6$
48	1.61	$> 10^6$
72	1.69	$> 10^6$
96	1.74	$> 10^6$
120	1.80	$> 10^6$
144	1.85	$> 10^6$
168	1.83	$> 10^6$
192	1.88	$> 10^6$
216	1.91	$> 10^6$
240	2.03	$> 10^6$
264	2.11	$> 10^6$
288	2.10	$> 10^6$
312	2.82	$> 10^6$
336	3.11	$> 10^6$